

LHCb/2007-010
TRACKING
April 23, 2007

VELO-TT track reconstruction

Olivier Callot

Laboratoire de l'Accélérateur Linéaire, Orsay, France

Marcin Kucharczyk, Mariusz Witek

Institute of Nuclear Physics PAN, Cracow, Poland

Abstract

The paper describes the track reconstruction in the system of VELO and TT detectors. Two separate algorithms for off-line and on-line approaches were merged. The single algorithm consists of the common code for pattern recognition and two parts specific to off-line and on-line functionalities. The note presents the performance in terms of track reconstruction efficiency and ghost rate.

Contents

1	Introduction	2
2	Pattern recognition	2
3	Simplified VELO-TT fit	5
4	The tuning for on-line reconstruction	6
5	The tuning for off-line reconstruction	7
6	Future development	8

1 Introduction

The reconstruction of short tracks in detectors situated before the magnet is of a specific nature. In the off-line environment the short tracks are searched for to recover the low momentum tracks which do not reach the T stations or are not reconstructed by the long track finding algorithms due to various reasons. The low momentum tracks are used in the method of global particle identification and may serve for flavour tagging, in particular if they are identified as kaons. It is possible that these short tracks can be used in the future for selecting some B decay channels. The momentum range concerned is 0.5-3 GeV/c.

In the trigger system, the main purpose of the VELO-TT reconstruction is to find high p_T tracks. The high p_T combined with the high impact parameter is the signature of B-decay products and can be used as a powerful tool to suppress the rate of minimum bias events coming from L0. The momentum range of tracks considered in the trigger is above 3 GeV/c.

So far two separate algorithms were employed: for the off-line [1] and on-line [2, 3]. Although the two algorithms refer to different momentum ranges and work within different environments and timing constraints, a single algorithm for both cases has been developed and is the subject matter of this note. A large part of the algorithm is the same for both cases. In particular, they both have an identical pattern recognition phase. The only difference is the tuning of steering parameters to fulfil the requirements of different momentum ranges. The following parts concern the selection of a unique track candidate, the determination of momentum and the requirements related to the track quality.

2 Pattern recognition

The input for pattern recognition is a collection of VELO tracks and a set of TT hits. The TT hits are created from the light clusters which are read out from the raw buffer. Every hit contains the information about the central point of the cluster (the barycenter of the TT cluster), readout strip length (the TT readout scheme is described in [4]) and the error on the coordinate perpendicular to strip orientation. The track finding makes use of two windows which are presented in Fig. 1. The first one is the *Search Window*, W_{search} , opened around the straight line extrapolation of the VELO track at z_{mid}^{tt} , the z coordinate in the middle of TT. This window is used to collect TT hits which might correspond to a given VELO track. The size of W_{search} depends on the minimum momentum of the track. The deflection from the straight line extrapolation, calculated at z_{mid}^{tt} as a function of inverse momentum, is shown in Fig. 2. Based on the hits falling into the search window the combinations of hits coming from a VELO track under consideration are constructed. The Δx is calculated for each layer as a difference between the x coordinate of the hit and the x coordinate of the straight line extrapolation of the VELO track. Δx is then rescaled to the z_{mid}^{tt} and is indicated by Δx^{norm} . To obtain a perfect VELO track, in the absence of multiple scattering, the correct hits should have the same value of Δx^{norm} .

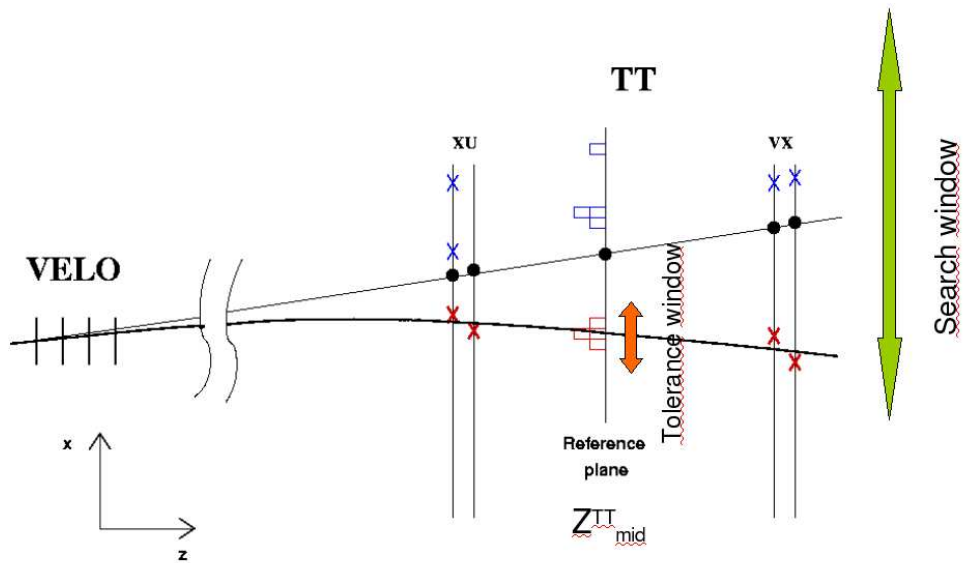


Figure 1: The idea of the pattern recognition in TT.

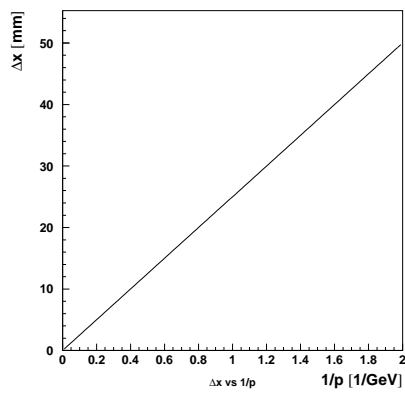


Figure 2: The expected deflection from the straight line in the magnetic field Δx , calculated in the middle of TT as a function of inverse momentum.

for the four TT layers. In a real situation a spread of these distances around some central value is expected. The *Tolerance Window*, W_{tol} , shown in Fig. 1 is employed to set the maximum allowed difference between the values of Δx^{norm} coming from different TT layers. The example distribution of the difference between the first and third TT layers, $\Delta x_1^{norm} - \Delta x_3^{norm}$, is illustrated in Fig. 3 for the two momentum ranges. According to the expectations, a much wider spread is observed for the low momenta due to a greater influence of multiple scattering. It is clear that the fixed value of the absolute difference $\Delta x_i^{norm} - \Delta x_j^{norm}$ (i, j denote the TT layers, $i \neq j$) cannot be used for the whole momentum range. However, the relative value

$$S_{rel} = (\Delta x_i^{norm} - \Delta x_j^{norm}) / \Delta x_i^{norm}$$

only weakly depends on the momentum of the track (Fig. 3). Thus the tolerance window can be expressed by the linear dependence valid for all the momenta:

$$W_{tol} = W_{tol}^0 + S_{rel} * \Delta x^{norm},$$

where W_{tol}^0 is the constant reflecting the spatial resolution within the limit of infinite momentum, while S_{rel} embraces effects of multiple scattering, increasing for low momenta. To speed up the procedure, the hits are sorted in the ascending order

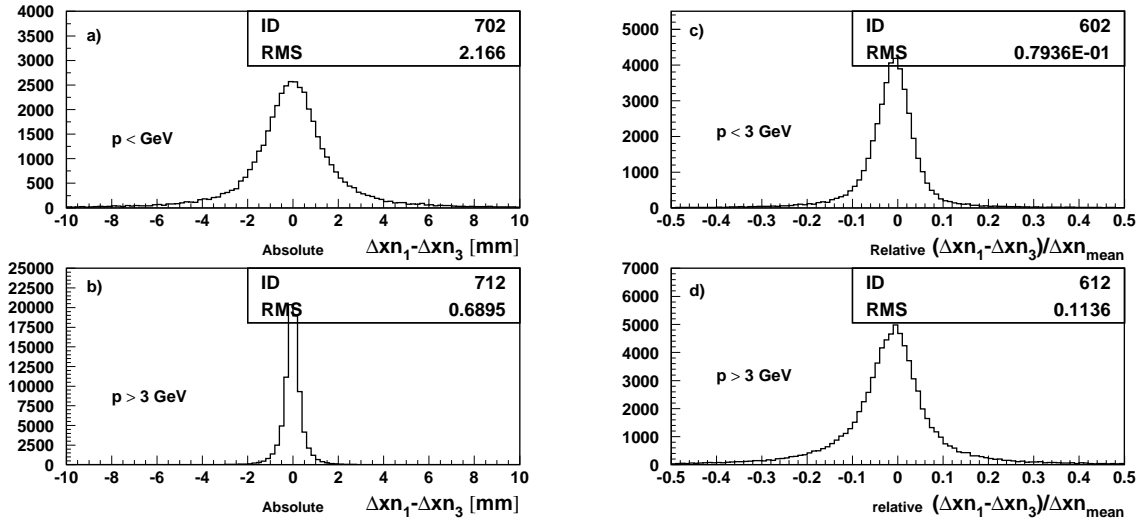


Figure 3: Distributions of absolute difference of normalized deflections Δx^{norm} between two TT layers on different stations for a) $p < 3$ GeV and b) $p > 3$ GeV. Distributions of a relative difference are shown for c) $p < 3$ GeV and d) $p > 3$ GeV. The width of relative distributions depends weakly on the momentum and can be used to fix the size of the tolerance window for all momenta.

according to their Δx^{norm} , from the smallest negative value to the largest positive one. The search for the combinations of TT hits is performed in turn for every

hit. Other hits are added to the combination if they are found within the tolerance window. The best combination has to be selected from the list of all of them. There are two different procedures for on-line and off-line cases, where the simple least square fit is an important element.

3 Simplified VELO-TT fit

The main reason behind the simplified VELO-TT fit is the limitation of the execution time. The Kalman fit based on the Transport Service could not be used in the environment of High Level Trigger. A dedicated least square fit was developed to determine the track momentum. The corresponding pseudo χ^2 can be used to select the best solution from the combinations of TT hits¹ found.

It is assumed that the track segments in VELO and TT can be approximated by straight lines which converge at one point. This condition is fulfilled in the case of VELO trajectory where the magnetic field is negligible. In the region of TT the approximation is still reasonable for the momenta above 3 GeV, i.e. for the range of concern for the HLT. In the case of lower momenta a bias is expected, due to a significant deviation from linearity which occurs in the increasing magnetic field in the TT region. However, this low momentum region is important for the off-line analysis and may be duly considered in the final stage by the Kalman fit. The two linear track segments in VELO and TT are supposed to meet at a point (x_{bdl}, z_{bdl}) in the XZ projection. The z_{bdl} indicates the z coordinate corresponding to a half of the Bdl integral (the middle of the effective magnet). Since there is no deflection in the YZ projection, the y slope in TT, s_y^{tt} , is assumed to be the same as s_y^{velo} . The total pseudo χ^2 consists of two elements:

$$\chi_{tot}^2 = \chi_{velo}^2 + \chi_{tt}^2,$$

where

$$\chi_{velo}^2 = \left(\frac{\Delta t_x^{velo}}{\sigma_{t_x^{velo}}} \right)^2 = f_1(x_{bdl})$$

and

$$\chi_{tt}^2 = \sum_{i=1}^n \left(\frac{\Delta x_i}{\sigma_{x_i}} \right)^2 = f_2(x_{bdl}, t_x^{tt}).$$

The first component χ_{velo}^2 comes from the uncertainty on the track slope measured in VELO. The second component is the χ^2 of the straight line in TT. As indicated above, the χ_{tot}^2 is a function of two unknown parameters, x_{bdl} and s_x^{tt} . The minimum of this two-dimensional function can be determined by solving the following system of equations:

$$\frac{\partial \chi_{tot}^2}{\partial x_{bdl}} = 0, \quad \frac{\partial \chi_{tot}^2}{\partial t_x^{tt}} = 0.$$

¹Since the errors used in the simplified fit do not include contribution from the multiple scattering, the χ^2 used for minimization is not statistically correct and therefore it is called pseudo χ^2 .

Since the solution can be expressed analytically, the execution of the algorithm is fast. The product of the inverse momentum and the charge of the track can be determined in the XZ projection according to:

$$\frac{Q}{p_{xz}} = 3.3356 * (\sin\theta_{tt} - \sin\theta_{velo}) / \int Bdl,$$

where θ_{tt} and θ_{velo} indicate angles of the track in the XY projection in TT and VELO, respectively. The pseudo χ^2 coming from the minimization will be denoted as χ_{pseudo}^2 .

The total momentum can be found using the slope of the track in the YZ projection.

$$p = p_{xy} * \sqrt{1 + (s_y^{tt})^2}.$$

4 The tuning for on-line reconstruction

As was explained in the note [5], the quality of the reconstruction is crucial for the performance of the generic $b\bar{b}$ trigger². The optimal working point is a compromise between good high p_T tracks efficiency (important for signal selection efficiency) and a low rate of low p_T tracks wrongly assigned to high p_T ones (reduction of minimum bias events).

Typically tracks with $p_T > 1$ GeV, are responsible for the trigger decision. Since $p = p_T / \sin\theta$, the momentum range of tracks with $p_T \geq 1$ GeV starts from ~ 3 GeV for highest θ measurable in LHCb and quickly goes up with decreasing θ angle. As can be seen in Fig. 2, the width of the search window used to reconstruct tracks with momenta above 3 GeV is around 10 mm. In the algorithm, the minimum momentum of the searched tracks is specified and then translated to the width of the W_{search} . The constant size, W_{tol}^0 , is set to 0.8 mm. This value was set by analysing the distribution of the Δx^{norm} for correct TT hits. It turned out that the momentum dependent term $S_{rel} * \Delta x^{norm}$ could be neglected since the reconstruction efficiency of high momentum tracks shows no significant improvement.

There might be a number of combinations of TT hits for a single VELO-TT track. A solution is chosen on the basis of the number of activated TT layers. The solution with more layers is favoured (4 layers vs 3 layers). In the case of equal number of layers the solution with smaller χ_{pseudo}^2 is preferred³.

The performance of the reconstruction is illustrated in Fig. 4. The two curves, for the signal efficiency and ghost rate as a function of momentum, correspond to the cut on maximum $\chi_{pseudo}^2 / NDF < 256$. For tracks with $p > 5$ GeV the average efficiency and ghost rate are 84.5 % and 4.8 % respectively.

²The trigger performance is defined as the signal efficiency at a fixed level of retention for minimum bias events.

³Usually, it involves selection of a higher momentum track.

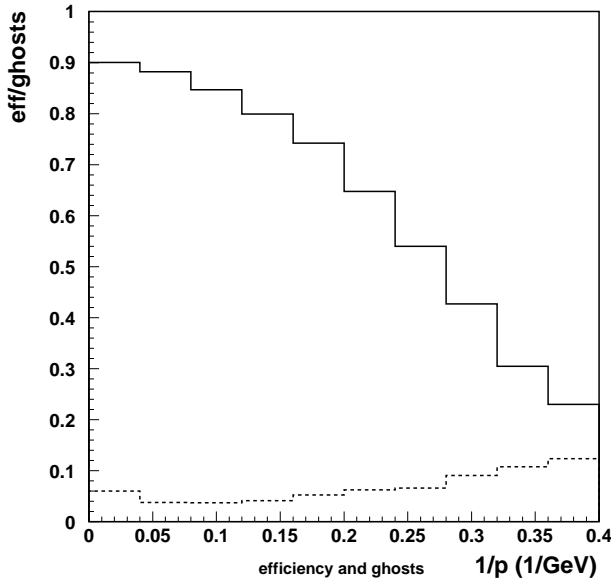


Figure 4: Track reconstruction efficiency (solid line) and ghost rate (dashed line) after the on-line tuning.

5 The tuning for off-line reconstruction

In the case of off-line reconstruction the selection of unique combination of TT hits associated to a given VELO track is based on the χ^2 of the Kalman fit. This enables a correct comparison of the track quality over the whole range of track momenta. One disadvantage is the large CPU time needed to fit all VELO-TT track candidates. For VELO tracks pointing to regions of high hit density the number of candidates to be considered can be large. Therefore a preselection of combinations based on the χ_{pseud}^2 coming from the simple fit (Sec. 3) is performed. The three track candidates having smallest χ_{pseud}^2 are kept for the Kalman fit. The single combination with the lowest χ^2/NDF is kept. The removal of VELO-TT track candidates sharing the same TT hits is done in the same way as in on-line mode⁴. The distributions of χ^2/NDF from the the Kalman fit for correctly and wrongly matched TT hits are shown in Fig 5. Tracks with $\chi^2/NDF > 5$ are removed.

The performance for the reconstruction in off-line mode is shown in Fig 6. The efficiency and ghost rate curves correspond to pattern recognition starting from all VELO tracks and all TT hits. For tracks with $p > 1$ GeV the average efficiency and ghost rate are 85.6 % and 15.5 % respectively.

For the sequence of reconstruction algorithms in the Brunel the VELO-TT track finding is executed at the end of tracking. Many VELO tracks are already converted to long tracks and their momenta are precisely measured. Therefore, the VELO-

⁴The real χ^2 is used instead of χ_{pseud}^2 .

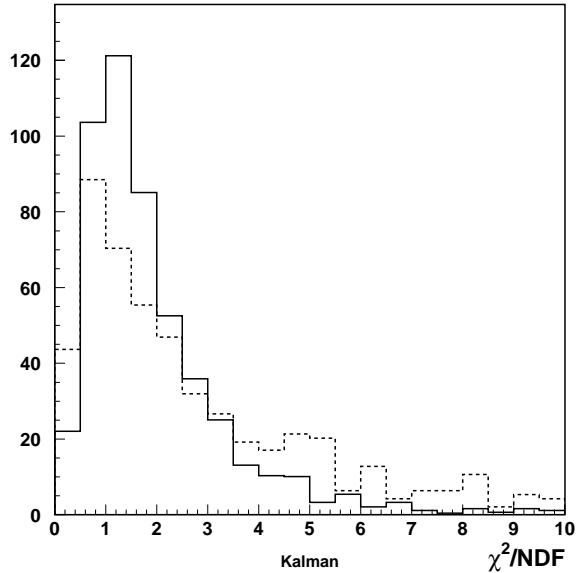


Figure 5: The distribution of the χ^2 after the fit for correct (solid line) and wrong (dashed line) Velo-TT matching. The distributions are normalized to the same area.

TT reconstruction needs only to be performed for the VELO tracks which were not reconstructed by other tracking algorithms. In addition only the TT hits which were not associated to any track should be used. The efficiency and ghost rate for such initial conditions are presented in Fig 7 as a function of momentum. One can see that the ghost rate becomes very high for momenta below 1 GeV. Since multiple scattering washes out the difference between correct and incorrect track candidates the reconstruction quality cannot be significantly improved.

6 Future development

The current version of VELO-TT reconstruction, described in this note, is used in two applications: Brunel (off-line tuning) and HLT (on-line tuning). There is still room for modifications. In the off-line case two improvements have to be implemented. The track state at the end of VELO has to be used, rather than the state closest to the beam.

It is necessary to use the Kalman fit for all TT combinations in order to select the best solution. This will be possible when the new fast Transport Service is available. In the case of the on-line version, a major technical rebuild of the algorithm is foreseen⁵. The current algorithm for pattern recognition, track fit and momentum determination will be split into three parts: the common code will be put into

⁵It will affect the off-line version too.

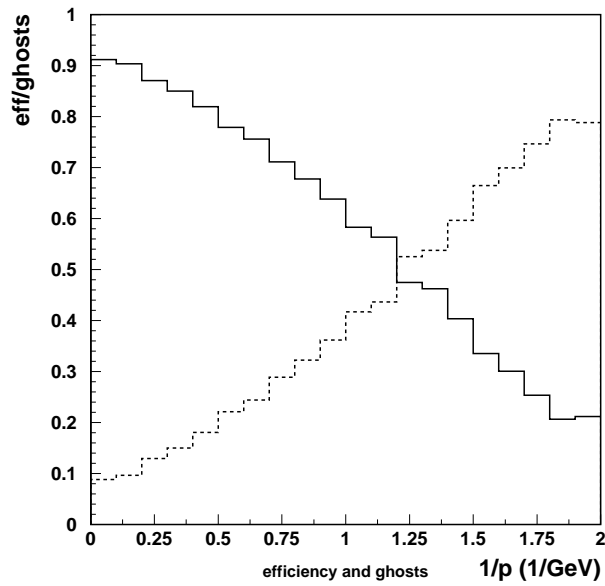


Figure 6: Track reconstruction efficiency (solid line) and ghost rate (dashed line) as a function of inverse momentum after the off-line tuning.

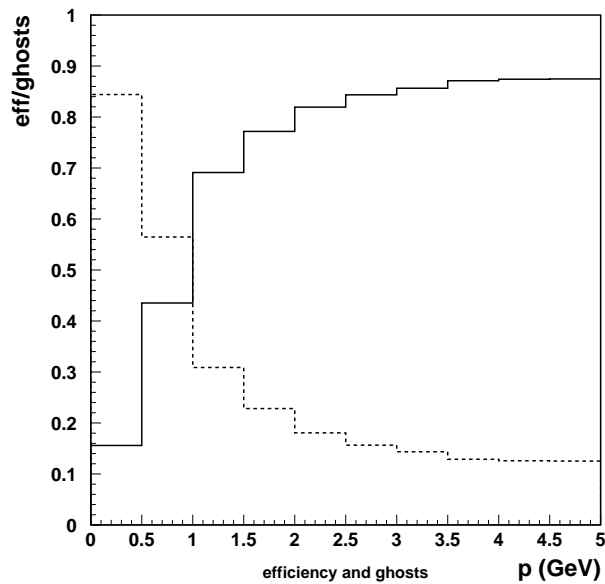


Figure 7: Track reconstruction efficiency (solid line) and ghost rate (dashed line) as a function of momentum for the tracks that are not reconstructed in the T stations.

the Gaudi tool and specific short algorithms will be created for off-line and on-line applications.

Such a modification will not affect the performance described in the present note. However, it will allow for the introduction of a better structure of the HLT algorithm where the different treatment of selected tracks has to be considered within the new trigger structure which is based on the idea of alleys.

At the same time a modification of the pattern recognition to run with no magnetic field is being implemented.

References

- [1] *Short track reconstruction with VELO and TT*, Y. Xie, Note LHCb-2003-100.
- [2] *VELO-TT matching and momentum determination at Level-1 trigger*, M. Witek, Note LHCb-2003-060.
- [3] *Online Pattern Recognition*, O. Callot, Note LHCb 2004-094.
- [4] *Channel Numbering and Readout partitioning for the Silicon Tracker*, M. Needham, Note LHCb-2006-033.
- [5] *The relevance of the magnetic field in the Level-1 trigger*, H. Dijkstra, J. A. Hernando, T. Schietinger, M. Witek, Note LHCb-2003-110.